Impaired spermatogenesis, tubular wall disruption, altered blood-testis barrier composition and intratubular lymphocytes in an infertile Beagle dog – a putative case of autoimmune orchitis

Carolin Matschurat[1], Kristina Rode[1], Julia Hollenbach[2], Karola Wolf[3], Carola Urhausen[3], Andreas Beineke[4], Anne-Rose Günzel-Apel[3] and Ralph Brehm[1]

[1]Institute for Anatomy, University of Veterinary Medicine Hannover, [2]Institute of Functional and Applied Anatomy, Hannover Medical School, [3]Unit for Reproductive Medicine - Small Animal Clinic, University of Veterinary Medicine Hannover and [4]Department of Pathology, University of Veterinary Medicine Hannover, Hannover, Germany

Summary. Impairment of blood-testis barrier integrity can be observed during inflammation, infection, trauma and experimental autoimmune orchitis, which is inducible in rodents. In the present study, an initially fertile two-year-old Beagle dog was presented with a decline in total sperm number resulting in azoospermia within five months, verified by twice-monthly semen analyses. The dog was clinically healthy with bilateral small testes and showed normal thyroid function. Bacterial cultures of semen were negative and serum biochemical analyses showed no abnormal findings. To determine causes of azoospermia, the dog was castrated. Histological examinations of hematoxylin-eosin stained testicular sections revealed impaired spermatogenesis, seminiferous tubules with spermatogenic arrest or Sertoli-cell-only syndrome as well as focal interstitial and even intratubular lymphocytic infiltrations. Germ cell sloughing, apoptosis and giant cells were also observed in some tubules. Subsequent immunostainings of smooth-muscle-actin, claudin3, claudin11 and connexin43 demonstrated, for the first time, a mechanical and functional disruption of the tubular wall and alterations of blood-testis barrier proteins in these tubules. Presence of claudin3 and claudin11 in canine testis was confirmed using RT-PCR and sequencing and/or Western-blot analyses. All findings suggested a possible spontaneous autoimmune orchitis to be the underlying cause for the observed azoospermia.

Key words: Autoimmune Orchitis, Blood-Testis Barrier, Claudins, Dogs, Testis

Introduction

The blood-testis barrier (BTB) represents a dynamic structure build up by tight junctions (TJ) and gap junctions (GJ) between adjacent Sertoli cells (SC), thus dividing the seminiferous epithelium into a basal and adluminal compartment (Cheng et al., 2010). This barrier ultimately preserves haploid germ cells (GC) from the blood and the autoimmune system (Stanton, 2016), and allows developing GC to enter the adluminal compartment for further differentiation by disassembling and reassembling junctional complexes (Meng et al., 2005).

Typical components of TJ are claudin-3 (CLDN3) and claudin-11 (CLDN11), whereas connexin-43 (CX43) is the predominant testicular GJ-protein (Pointis and Segretain, 2005). So far, only occludin (OCLN; Gye, 2004) and CX43 (Ruttinger et al., 2008) have been identified as components of the canine BTB.

In addition, within the dog testis, there exists a close morphofunctional relationship and crosstalk between the tubular wall, its basement membrane, peritubular myoid

cells and SC. However, canine contractile cells do not represent such an impediment in dogs as reported for laboratory rodents. This is congruent with the situation in other domestic mammals as the basement membrane only seems to delay (and not stop) the passage of lanthanum tracer in dogs (Cambrosio Mann et al., 2003). The basement membrane contains, for example, pools of cytokines, which are known regulators of SC function, such as BTB formation and integrity (Cheng et al., 2010).

The pathogenesis of autoimmune orchitis (AIO) is still unknown. Although the etiology is likely to be multifactorial, it was shown that testicular inflammation or trauma is able to induce T-cells to produce pro-inflammatory cytokines which in turn can induce alterations of BTB permeability or modifications of the normal testicular environment (Hedger and Meinhardt, 2003; Fijak and Meinhardt, 2006; Silva et al., 2014; Perez et al., 2014). Impairment of BTB integrity has, for example, been observed in rats during inflammation, infection, trauma and AIO (Fijak et al., 2005). Furthermore, AIO is characterized by an autoimmune testicular inflammation that may lead to infertility with possible presence of antisperm-antibodies (Casal, 2012). AIO and lymphocytic orchitis are very rarely described in dogs and may be under-diagnosed due to non-specific clinical signs and lack of diagnostic tools (Fritz et al., 1976; Olson et al., 1992; Casal, 2012; Silva et al., 2014; Davidson et al., 2015; Donnelly et al., 2016). However, dogs (and minks) are species in which spontaneous AIO has been shown to occur (Allen and Longstaffe, 1982; Casal, 2012).

In contrast, experimental autoimmune orchitis (EAO) is a well-established model for understanding possible causes of AIO and is inducible in rodents (Fijak et al., 2005). Histological findings include interstitial lymphocytic infiltration, apoptotic GC and GC-sloughing within the tubular lumen (Perez et al., 2012). Moreover, affected seminiferous tubules show maturation arrest at the level of spermatogonia, spermatocytes or round spermatids, and Sertoli-cell-only syndrome (SCO) (Naito et al., 2012). Intraepithelial lymphocytes are not present in "normal" seminiferous epithelium except very close to the junction of the seminiferous tubules with the tubuli recti (Dym and Romrell, 1975; Naito et al., 2012).

Material and methods

Case report

In this case report, an initially fertile two-year-old Beagle dog weighing 18.5 kg was presented with a progressive decline in total sperm number resulting in azoospermia within five months, verified by twice-monthly semen analyses performed for teaching purposes (Fig. 1). Throughout the investigated period, the dog was clinically healthy, but morphological examinations manifested bilateral soft and small testes

(length x width: 2.7 cm x 1.7 cm) in relation to the bodyweight (mean length x width for dogs of 10-20 kg: 3.5 cm x 2.4 cm (Günzel-Apel and Bostedt, 2016). Ultrasonographically, both testes showed focal hyperechoic areas, whereas the epididymides and prostate appeared normal. No causal trigger like trauma, torsion or illness was reported. Diagnostic work-up of testicular atrophy and azoospermia by bacterial culture of semen, including mycoplasma as well as hematological and serum biochemical analyses, revealed no alterations. Furthermore, the antibody titer against canine herpesvirus was low, though did not rule out a possible and causal viral infection. Hypothyroidism was ruled out by thyroxine and thyroglobulin values, which were within the reference range. During semen collection, the dog showed good libido and normal mating-behavior. After having reached the infertile stage due to azoospermia, the dog continued to be kept for research and teaching purposes for two more years before castration was performed.

Samples and hematoxylin-eosin (HE) staining

Both testes were collected during routine castration, fixed in Bouin's solution and embedded in paraffin using standard techniques. Additionally, testicular samples of two adult dogs (a Labrador retriever and a Beagle dog) showing normal spermatogenesis were snap-frozen in liquid nitrogen and stored at -80°C for reverse transcription-PCR (RT-PCR) and Western-blot analysis (WB), serving as controls. For histological evaluation, 3-4 μm sections of all samples were stained with HE using standard protocols.
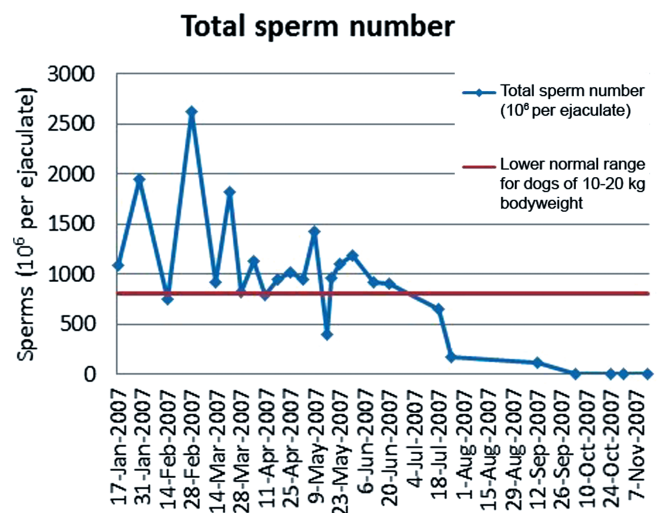

Total sperm number

Fig. 1. Total sperm number per ejaculate over time. Progressive decline in total sperm number resulting in azoospermia.

Immunohistochemistry (IHC)

Assessment of BTB: claudin-3 (CLDN3), claudin-11 (CLDN11), connexin-43 (CX43) and smooth-muscle-actin (SMA)

To examine a possible disruption of the tubular wall and/ or changes in the distribution pattern of BTB proteins, especially seminiferous tubules showing intratubular lymphocytes, IHC on 3 μm serial sections was performed using specific antibodies against CLDN3, CLDN11, CX43 and SMA, summarized in Table 1.

For this purpose, deparaffinized and rehydrated sections were heat-treated in sodium citrate buffer (pH 6) at 96-99°C for 20 minutes for antigen retrieval, followed by blocking with 3 % of bovine serum albumin (BSA) in PBS at room temperature for 20 minutes (SMA without antigen retrieval and with 20 % of normal goat serum in PBS instead of BSA for blocking). Sections for CLDN3 were stained using the avidin-biotin-enzyme complex (ABC) method (Vectastain Elite ABC-standard-kit, Vector Laboratories). All sections were incubated with the corresponding primary antibody at 4°C overnight in a humid chamber.

On the following day, sections were exposed to the compatible secondary antibody for 30 minutes (CLDN11, CX43 and SMA) or to the biotinylated secondary antibody for 45 minutes (CLDN3), the latter followed by incubation with ABC for 30 minutes, and enhancement reaction with biotinylated tyramine in PBS for 15 minutes at room temperature. Afterwards, CLDN3 sections were incubated again with ABC for 15 minutes.

Immunoreactivity of all sections was visualized by the diaminobenzidine detection system (DAB) and sections were counterstained with hematoxylin. Non-specific binding of the primary antibody was assessed by rabbit or mouse IgG-isotype control, respectively.

Assessment of lymphocytes: CD3 and PAX5

For further characterization of infiltrating lymphocytes, a CD3-specific antibody and a PAX5-specific primary antibody were used for detecting T-cells and B-cells, respectively (see Table 1). Antigen identification was performed by the ABC method. Paraffin embedded tissues were deparaffinized in Roticlear (Carl Roth GmbH, Karlsruhe, Germany) and rehydrated through graded alcohols. Endogenous peroxidase activity was suppressed with 0.5 % H_2O_2 in methanol, followed by incubation with primary antibody overnight at 4°C. Specificity controls included substitution of the monoclonal antibody with ascitic fluid from nonimmunized BALB/cJ mice or rabbit normal serum was used. Spleen tissue of a healthy dog was used as positive control for detecting T- and B-cells (data not shown).

Incubation with primary antibodies was followed by incubation with corresponding biotinylated secondary antibodies for 30 minutes at room temperature. Subsequently, ABC (Vectastain Elite ABC Kit; Vector Laboratories, PK 6100, Burlingame, CA) was added and incubated for 30 minutes at room temperature. Antigen-antibody reactions were visualized by incubation with DAB for 5 minutes, followed by counterstaining with hematoxylin.

RT-PCR of CLDN3 and -11 mRNA expressions in canine testis

RNA extraction, DNase treatment and cDNA synthesis

RT-PCR was performed with whole testis homogenate of two adult dogs with normal spermatogenesis to analyze and confirm testicular CLDN3 and CLDN11 mRNA-expression. Total RNA was isolated using TRIzol® reagent (Ambion Life

Table 1. Antibodies used for immunohistochemistry (+) and Western blot analysis (++).

Corresponding protein	Primary antibody	Catalog no.	Source	Dilution	Secondary Antibody
β-actin (++)	β-Actin antibody	sc-47778	Santa Cruz Biotechnology, USA	1:5000	Goat anti-mouse HRP antibody, Santa Cruz Biotechnology, USA
CD3 (+)	Anti-human CD3	A0452	Dako, Denmark	1:200	Biotinylated goat anti-rabbit IgG, Vector Laboratories, USA
Claudin-3 (+)	Anti-Claudin-3	34-1700	Invitrogen Corporation, CA, USA	1:500	Labelled Polymer-HRP anti-rabbit, Dako, North America
Claudin-11 (+)	Anti-oligodendrocyte antibody	ab53041	Abcam plc, Cambridge, UK	1:3000	Labelled Polymer-HRP anti-rabbit, Dako, North America
Claudin-11 (++)	Anti-Claudin-11 antibody	CPA1843	Cohesion Bioscience, London, UK	1:2000	Goat anti-rabbit HRP antibody, Santa Cruz Biotechnology, USA
Connexin-43 (+)	Connexin 43 antibody	3512	Cell Signaling Technology, MA,USA	1:500	Labelled Polymer-HRP anti-rabbit, Dako, North America
Pax5 (+)	Mouse anti-Pax-5	610863	BD Transduction laboratories, KY, USA	1:500	Biotinylated, goat anti-mouse IgG, Vector Laboratories, USA
Smooth-muscle-actin (+)	Anti-human Smooth Muscle Actin	M0851	Dako, Denmark	1:500	Labelled Polymer-HRP anti-mouse, Dako, North America

technologies, Karlsruhe, Germany) in accordance with the manufacturer's protocol. After RNA quantification by spectrophotometry at 260 nm (DeNovix® DS-11, DeNovix Inc., Wilmington, USA), 10 μg of total RNA was incubated with DNase (DNase I recombinant, Roche Diagnostics, Mannheim, Germany) to digest genomic DNA. Afterwards, cDNA synthesis from 2 μg of total RNA was performed using MultiScribe Reverse Transcriptase (Applied Biosystems, California, USA) as recommended by the manufacturer.

RT-PCR

Specific PCR-primers for canine CLDN3 and -11 were designed using the PubMed Primer-designing-tool (Table 2) and purchased from Eurofins Scientific (Ebersberg, Germany).

For RT-PCR, 2 μl cDNA (for CLDN3) or 1 μl cDNA (for CLDN11) was added to 24 μl PCR master mix (15 μl diethyl pyrocarbonate water (DEPC), 5 μl 5x Green GoTaq Buffer, 2 μl MgCL2, 0.5 μl dNTP, 0.5 μl forward primer, 0.5 μl reverse primer and 0.5 μl GoTaq Flexi DNA polymerase (Promega, Madison, Wisconsin, USA). DEPC water was used instead of RNA as a no-template control. PCR amplification was conducted using PCR standard protocols. Amplified fragments were separated on a 2% agarose gel and bands were visualized with GelRed Nucleic Acid Stain (Biotrend Chemikalien, Cologne, Germany).

The PCR-products were isolated using the GeneJET Gel Extraction Kit (Fermentas, St. Leon-Rot, Germany) and sequenced by Seqlab sequencing service (Seqlab Sequence Laboratories, Göttingen, Germany).

Qualitative WB-analysis

To confirm the specificity of CLDN11-antibody and immunohistochemical data in canine testicular tissue, qualitative WB-analysis was performed. For this, protein extraction was carried out using TRIzol® reagent (Ambion Life technologies, Karlsruhe, Germany) in accordance with the manufacturer's protocol on frozen testicular samples of the same dogs used for RT-PCR. To determine protein concentrations, the DC protein Assay Kit (BioRad Laboratories, Munich, Germany) was used.

For electrophoresis, 20 μg protein homogenate was loaded per lane and then fractionated for 80 minutes by SDS-PAGE in a 15% polyacrylamide gel at 130 V. Afterwards, proteins were blotted onto a nitrocellulose blotting membrane (Amersham Protran, GE-Healthcare, Germany) for 60 minutes at 1 A/cm^2 (PeqLab, Erlangen, Germany). Subsequently, the membrane was blocked with 5% skimmed milk in Tris-buffered saline (TBS) and Tween-20 for 60 minutes, followed by incubation with rabbit anti-claudin-11 antibody overnight at 4°C (for antibodies, see Table 1). For negative controls, the primary antibody was omitted and replaced by TBS with Tween-20.

Next day, the membrane was incubated with the corresponding secondary antibody for 45 minutes at room temperature. Immunoreactive bands were detected using the SuperSignal West Dura Kit (ThermoFisher Scientific, Schwerte, Germany) following the manufacturer's protocol.

After stripping the membrane (0.2 M Glycin, Tween-20 and SDS) for 45 minutes, a loading control with β-actin (ACTB) and corresponding secondary antibody was performed using the same protocol.

Results

HE-staining

Histological examination revealed impaired spermatogenesis, focal peritubular and even intratubular lymphocytic infiltrations (Figs. 2a,c, 3a), arrest of spermatogenesis at different levels (Fig. 2a,e) and SCO-tubules (Fig. 2a,d), a phenomenon called mixed atrophy. Giant cells (Fig. 2e), apoptosis (Fig. 2b), vacuoles and GC-sloughing (Fig. 2a) were also observed in some tubules. There was complete absence of sperm in the epididymides and ductus deferentes (data not shown).

IHC

CLDN3, CLDN11, CX43 and SMA

IHC of SMA revealed annular staining patterns, but tubules with lymphocytic infiltrations showed interruptions (Fig. 3l). Blood vessels were also immunopositive and served as an additional internal positive control within the same section.

The staining pattern of CLDN3 was heterogeneous. Some tubules revealed an almost continuous belt at the basal BTB region, whereas other tubules showed luminal staining. In those tubules infiltrated with lymphocytes, immunostaining for CLDN3 was found to be diffuse and cytoplasmic (Fig. 3c). A specific staining in canine epididymis was detected apically between adjacent principal cells (data not shown).

CX43-IHC resulted in a specific staining belt at the basal region of the seminiferous tubules, corresponding to the known localization of CX43 at the BTB. However, tubules infiltrated with lymphocytes showed a discontinuous and delocalized immunostaining with

Table 2. Primer pairs used for specific amplification of claudin-3 and -11 (*Canis lupus familiaris*).

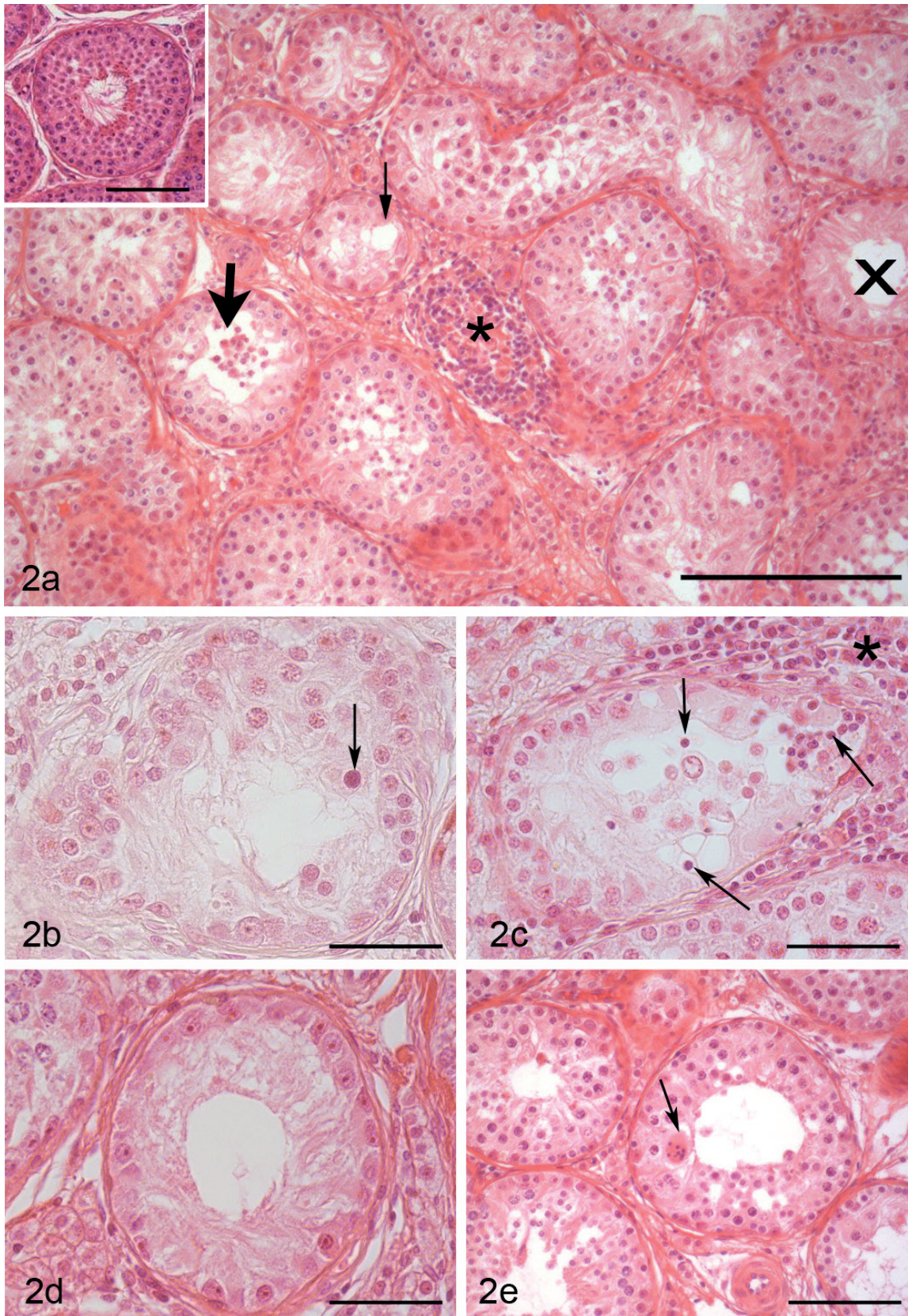| Claudin-3	(GenBank accession number: NM_001003088)
Forward primer:	5'- CATCCGGGACTTCTACAACCC -3'
Reverse primer:	5'- GAGTAGACGATCTTGGTGGGC -3'
Size of amplification product:	171 base pairs
Claudin-11	(GenBank accession number: XM_545284.5)
Forward primer:	5'- TGCCTCAACGTAACGCATCT -3'
Reverse primer:	5'- GTTTGGAGAGTTTGGGGCCT -3'
Size of amplification product:	164 base pairs

Fig. 2. Impairment of spermatogenesis, testis, dog. Representative HE-staining. **a.** Mixed atrophy: arrest of spermatogenesis at different levels, peritubular lymphocytic infiltration (star), vacuole (arrow), Sertoli-cell-only tubule (cross), germ-cell-sloughing (bold arrow). Inset showing normal spermatogenesis of a control dog. **b.** Germ cell apoptosis (arrow). **c.** Peritubular (star) and intratubular lymphocytic infiltration (arrows). **d.** Sertoli-cell-only tubule. **e.** Arrest of spermatogenesis, giant cell (arrow). Scale bars: a, 200 μm; b-d, 50 μm; e, inset, 100 μm.
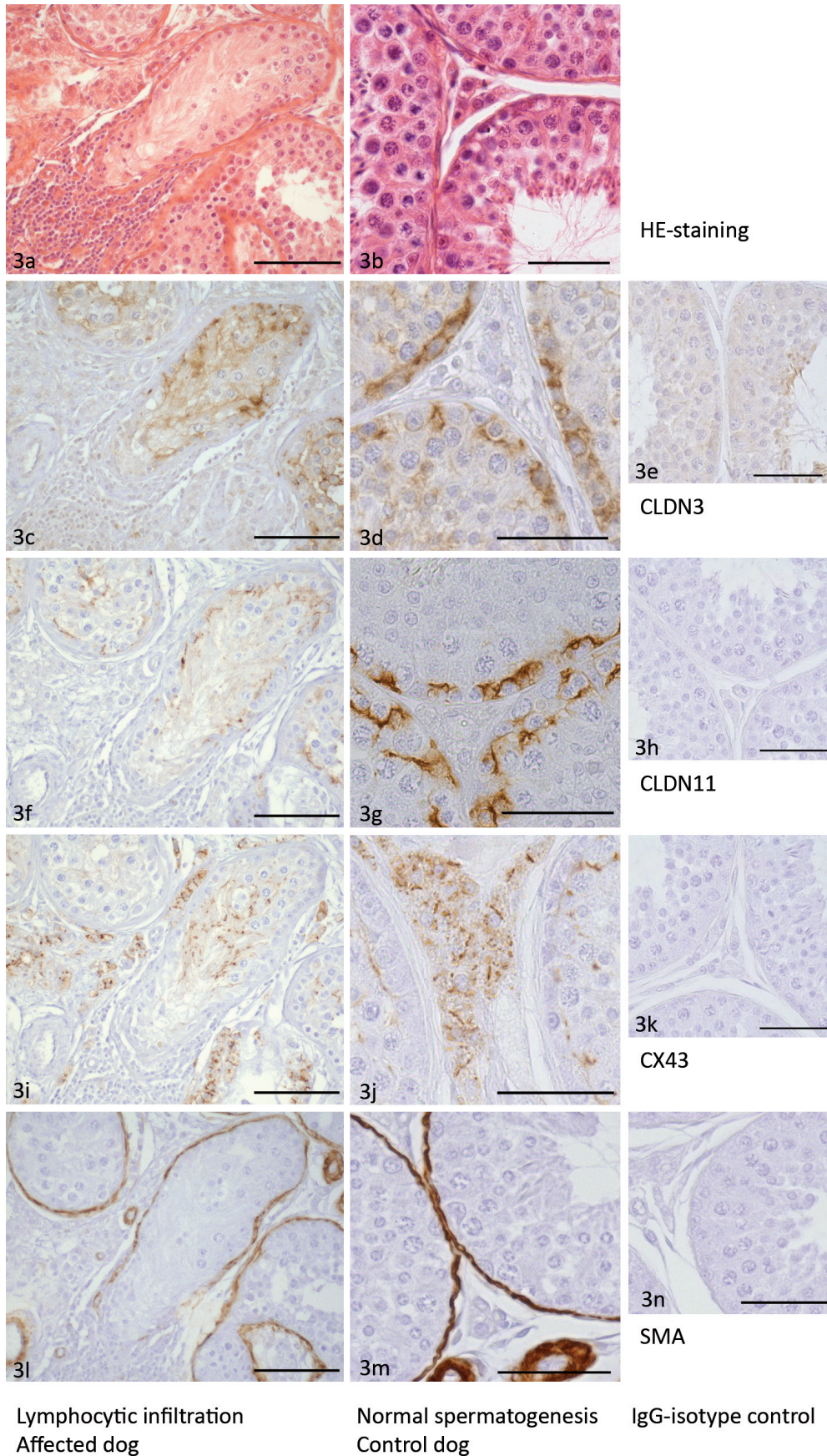
Fig. 3. Left hand side: intratubular lymphocytic infiltration, testis, affected dog. Centre and right hand side: normal spermatogenesis, testis, control dog. **a.** Intratubular lymphocytic infiltration. HE-staining. **b.** Normal spermatogenesis. HE-staining. **c.** Diffuse, cytoplasmic staining pattern. IHC for CLDN3. **d.** Staining at BTB-localization. Positive control. IHC for CLDN3. **e.** Rabbit IgG-isotype control for CLDN3. **f.** Discontinuous staining belt. IHC for CLDN11. **g.** Staining above spermatogonia, between Sertoli cells. Positive control. IHC for CLDN11. **h.** Rabbit IgG-isotype control for CLDN11. **i.** Decrease in staining intensity and delocalization. Interstitial Leydig cells also stained, similar to control dogs. IHC for CX43. **j.** Staining at BTB-level. Interstitial Leydig cells also positive. Positive control. IHC for CX43. **k.** Rabbit IgG-isotype control for CX43. **l.** Discontinuous staining belt. Blood vessel walls also stained. IHC for SMA. **m.** Annular staining of the tubular wall. Positive control. IHC for SMA. **n.** Mouse IgG-isotype control for SMA. Scale bars: a, c, f, i, l, 100 μm; b, d, e, g, h, j, k, m, n, 50 μm.
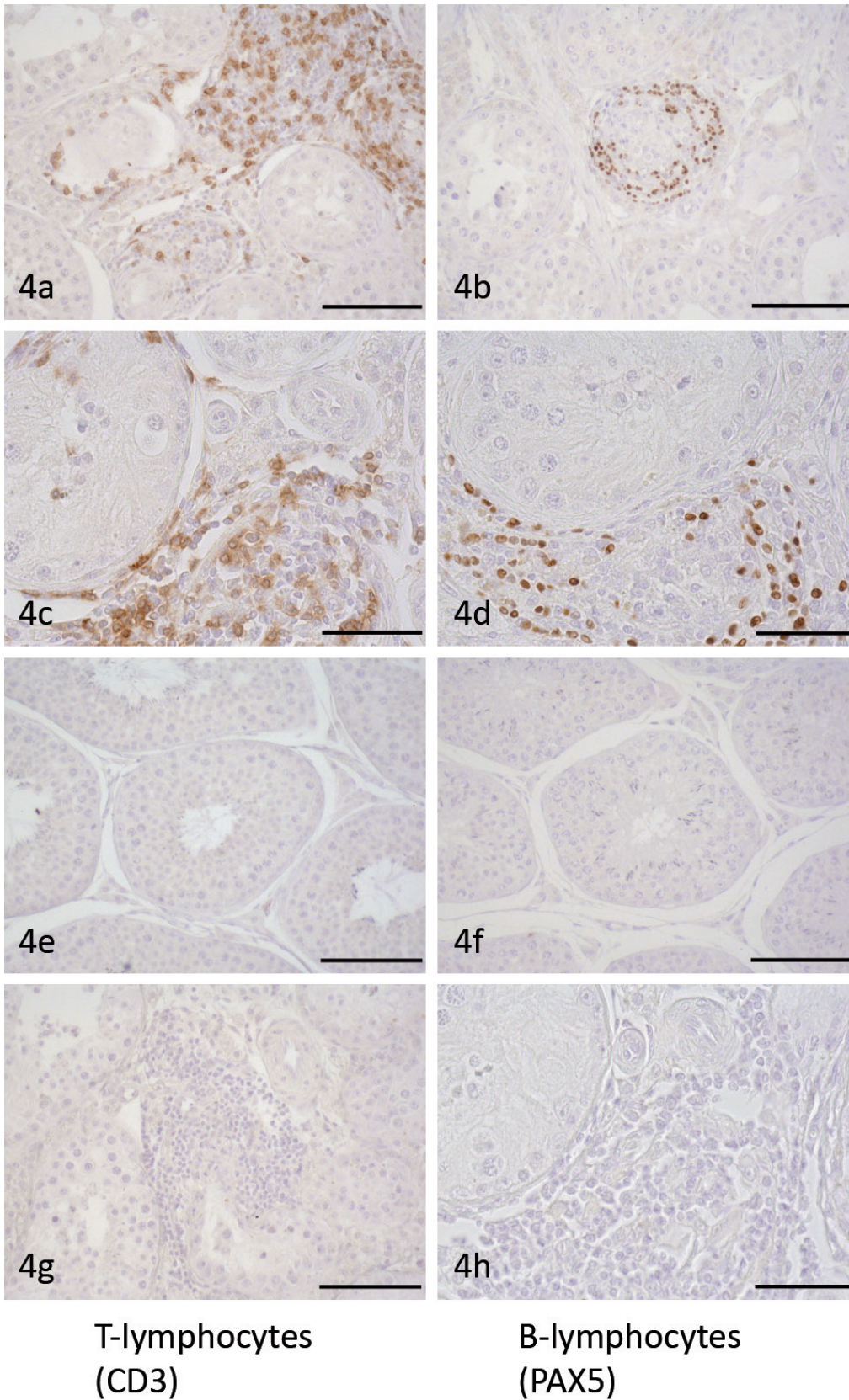
Fig. 4. Further investigation of infiltrating lymphocytes. IHC of canine testis. Left hand side: T-lymphocytes (CD3). Right hand side: B-lymphocytes (PAX5). **a, c.** T-lymphocytes infiltrating interstitium and tubules. CD3 positive staining of the affected dog's testis. **e.** No T-lymphocytes detectable in dogs showing normal spermatogenesis. **g.** Negative control of CD3. **b, d.** B-lymphocytes infiltrating the interstitium. PAX5 positive staining of the affected dog's testis. **f.** No B-lymphocytes detectable in dogs showing normal spermatogenesis. **h.** Negative control of PAX5. Scale bars: a, b, e-g, 100 μm; c, d, h, 50 μm.

T-lymphocytes
(CD3)

B-lymphocytes
(PAX5)

decreased immunoreactivity (Fig. 3i). Interstitial Leydig cells were also immunopositive, serving as an internal positive control.

Immunohistochemical detection of CLDN11 revealed a staining pattern within the basal compartment of the seminiferous epithelium. Some tubules with impaired spermatogenesis presented a stronger specific staining of the adluminal compartment, whereas tubules with lymphocytic infiltrations showed discontinuous staining belts, indicating alterations in BTB integrity and composition at these sites (Fig. 3f).

None of the IgG-isotype controls showed any specific immunostaining (Fig. 3e,h,k,n).

CD3 and PAX5

Both T-cells (Fig. 4a,c) and B-cells (Fig. 4d) were detected as involved lymphocytic subpopulations infiltrating the interstitium and tubules of the affected dog's testis using IHC of CD3 (T-cells) and PAX5 (B-cells). In dogs showing normal spermatogenesis, however, neither T-cells nor B-cells were identified (Fig. 4e,f). Negative controls did not show any specific staining (Fig. 4g,h).

RT-PCR

RT-PCR was performed to confirm immuno-histochemical data of CLDN3 and CLDN11 in canine testicular tissue at mRNA-level. Specific bands of 171 bp PCR-products for CLDN3 (Fig. 5, lanes 1, 2) and 164 bp for CLDN11 were detected (Fig. 5, lanes 1, 2). Sequencing of PCR-products confirmed the identity of canine CLDN3 and -11-mRNA. Negative controls did not show any specific amplification products (Fig. 5, lane 3).

WB-analysis

WB-analysis for CLDN11 detected a single immunoreactive band at approximately 22 kDa using

protein homogenates from two dogs with normal spermatogenesis (Fig. 6, lanes 1, 2). The negative control did not show any specific bands (Fig. 6, lanes 3, 4). Loading control with ACTB revealed immunorective bands at approximately 43 kDA (Fig. 6, lanes 1 - 4).

Discussion

AIO is rarely described in dogs (Fritz et al., 1976; Allen and Longstaffe, 1982; Casal, 2012; Davidson et al., 2015). In the present clinical case, testicular atrophy and a progressive decline in total sperm counts resulting in azoospermia occurred within a time period of five months, without any apparent signs of trauma or illness. Clinical examinations resulted in physiological findings. Histologically, a mixed atrophy as well as focal interstitial and intratubular lymphocytic infiltrations were detected. Using IHC, lymphocytes were characterized as T-cells and B-cells. Further signs indicating impaired spermatogenesis were visible with regards to apoptotic cells within the seminiferous epithelium and GC-sloughing. Finally, there was a complete absence of sperm in the epididymides. Histological findings were comparable to those known for spontaneous AIO or EAO (Doncel et al., 1989; Fijak et al., 2005; Perez et al., 2011; Naito et al., 2012).

To elucidate whether intratubular lymphocytic infiltrations are accompanied by a disruption of the tubular wall and with alterations in the distribution pattern and immunolocalization of BTB proteins, IHC was performed.

As previously described in normal adult dogs, CX43 staining was localized along the BTB and between Leydig cells (Ruttinger et al., 2008). However, in tubules infiltrated with lymphocytes, a discontinuous staining pattern with a reduced immunoreactivity could be detected. This was in accordance with results in rats
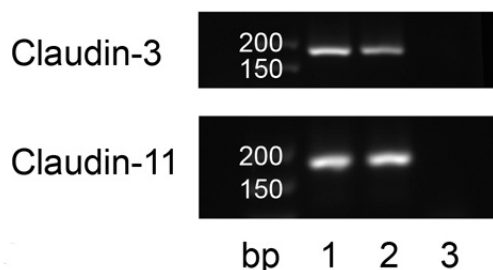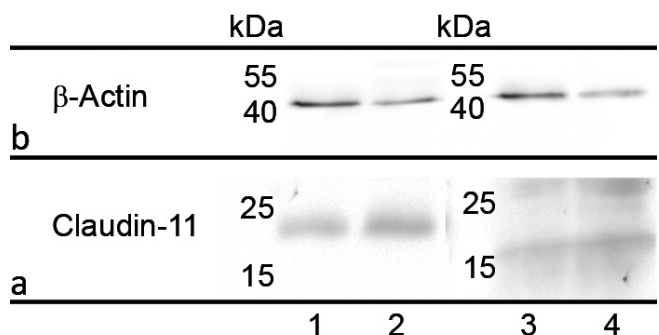

Fig. 5. RT-PCR analysis for CLDN3 and CLDN11 mRNA of testis homogenates from two adult dogs with normal spermatogenesis. Amplification products of 171 base pairs for CLDN3 (lanes 1 and 2) and 164 base pairs for CLDN11 (lanes 1 and 2) could be detected. Negative controls did not show amplification products (lane 3).

Fig. 6. a. Western-blot analysis for CLDN11 using protein homogenate from two adult dogs showing normal spermatogenesis. This revealed an immunoreactive band at 22 kDa (lanes 1 and 2). Corresponding negative controls only showed non-specific bands (lanes 3 and 4). **b.** Immunoreactive bands at 43 kDa could be detected using ß-Actin as loading control (lanes 1-4).

undergoing EAO, which also showed reduced expression of CX43 (Perez et al., 2011). Furthermore, it was demonstrated in mink testis, that AIO modifies CX43, therefore suggesting changes in CX43-mediated intercommunication and spermatogenic activity probably in response to cytokine imbalances in SC (Pelletier et al., 2011). These data support the idea of AIO as a possible underlying cause for azoospermia and infertility also in the presented Beagle dog.

The staining pattern of the TJ-protein CLDN3 was heterogeneous, both basally and adluminally. In mice, expression of CLDN3 is stage-specific to enable migration of preleptotene/ leptotene spermatocytes across the BTB (Smith and Braun, 2012; Chihara et al., 2013). A stage-specific expression of CLDN3 has not been reported in dogs yet, but data from dogs with normal spermatogenesis collected in this study indicated comparability with those derived from mice. Canine CLDN3-expression is described, especially for carcinomas of the mammary gland (Jakab et al., 2008; Hammer et al., 2016) and the gastrointestinal tract (Ohta et al., 2011). In infiltrated tubules, the distribution pattern of CLDN3 was discontinuous, again suggesting alterations in the BTB. In addition, a specific immunoreaction for CLDN3 was detectable in the epididymis, comparable to results derived from rats, apically between adjacent principal cells (Gregory and Cyr, 2006; Cyr et al., 2007). Using RT-PCR, the presence of CLDN3-mRNA was demonstrated for the first time in canine testis showing normal spermatogenesis.

In mice, deficiency of CLDN11 results in the loss of the SC epithelial phenotype, a disruption of BTB integrity and sterility, indicating that this TJ-protein is essential for normal spermatogenesis (Gow et al., 1999; Mazaud-Guittot et al., 2010). Also in human testis, CLDN11 represents an essential component of the BTB (Stammler et al., 2016).

Canine CLDN11 was mainly detectable in the basal compartment of the normal seminiferous tubules. Infiltrated tubules showed discontinuous staining belts, whereas a delocalized and increased staining intensity was observed in tubules with impaired spermatogenesis. In men affected by testicular intraepithelial neoplasia (TIN), the BTB was found to be disrupted. In addition, this impairment was related to disorganization or dysfunction of CLDN11 and not to a failure of CLDN11-expression (Fink et al., 2009). Furthermore, dislocalization of CLDN11 could be observed in rats undergoing EAO (Perez et al., 2012). The present findings for testicular CLDN11 also indicate a possible overexpression and dislocalization of this TJ-protein in dogs, especially in tubules showing impaired spermatogenesis, again suggesting a possible AIO to be the underlying cause. The immunohistochemical findings were confirmed by expression of CLDN11-mRNA via RT-PCR and sequencing. For the first time, canine CLDN11-protein was successfully identified by WB-analysis.

A mechanical and functional alteration of the tubular wall could be demonstrated by interrupted staining patterns of SMA in tubules with intratubular lymphocytic infiltrations (Egger and Witter, 2009).

For differential diagnoses of (canine) azoospermia, inherited or acquired diseases should be taken into consideration (Memon, 2007; Hesser and Davidson, 2015; Günzel-Apel and Bostedt, 2016). As the investigated dog was initially fertile, congenital illnesses like testicular hypoplasia or hypoplasia of the epididymis could be ruled out. Acute orchitis normally occurs due to an infection with pathogenic agents either after a traumatic insult or by hematogenic or ascending spreading, and is associated with a reduced general health condition. In the present case, no signs of acute orchitis were reported. Bacterial semen examinations including mycoplasma testing were also negative. Avascular injuries like torsion or trauma as underlying causes for azoospermia were also not reported. Chronic orchitis as a result of a subclinical bacterial infection often remains undetected as libido and mating behavior remain unaffected. Unevenly distributed hyperechoic spots would be conspicuous in the ultrasound, as would reduced testicular size, rough consistency and azoospermia (Günzel-Apel and Bostedt, 2016). As stated above, no evidence of a bacterial infection was found. Finally, testicular tumors like seminoma also result in impaired spermatogenesis and correlate with lymphocytic infiltrations (Grieco et al., 2004). No indication of testicular neoplasia was found histologically in the present case. However, as a low antibody titer of canine herpes virus was detected, a possible viral infection cannot be totally ruled out (Günzel-Apel and Bostedt, 2016).

In the present case study, accurate histological examination along with the immunohistochemical results for SMA, CLDN3, CLDN11 and CX43 demonstrated an interesting testicular phenotype, therefore suggesting AIO to be the underlying cause of impaired spermatogenesis and azoospermia. Seminiferous tubules with lymphocytic infiltrations showed a disruption of the tubular wall and alterations in the distribution pattern of different BTB proteins, which probably led to the presence of intraepithelial lymphocytes. Unfortunately, testicular tissue samples obtained either from castration or biopsy can only allow a "snap-shot" or histological description of a certain time-point. Thus, it remains open and has yet to be elucidated whether the observed alterations in the tubular wall and in BTB composition in infiltrated tubules were the cause or the consequence of migrating lymphocytes.

In any case, the role of intraepithelial lymphocytes in the pathogenesis of AIO of the testis remains unclear. However, it has been suggested that sensitized lymphocytes cause the initial damage to the seminiferous epithelium without prior presence of antisperm-antibodies (Tung et al., 1971; Dym and Romrell, 1975). In this context, it was further shown that

T-cells are generally able to induce alterations of blood brain barrier proteins like CLDN5 and occludin (Suidan et al., 2008). Finally, the cytokine IL17A released from T-helper-cells was able to impair BTB integrity and to induce testicular inflammation (Perez et al., 2014).

Taken as a whole, the detailed history of the dog, results of the physical examination and the examination of the reproductive tract, results from the semen evaluation as well as from the testicular histology and immunohistochemistry point to the diagnosis AIO. AIO in dogs is a disease that is still poorly understood and up to now, only few publications are available dealing with canine AIO. Thus, this case report may represent a valuable histological contribution to canine male reproductive research. Results might finally help to understand the pathophysiology and potentially inciting causes of this rare or underdiagnosed cause of infertility in male dogs.

References

Allen W.E. and Longstaffe J.A. (1982). Spermatogenic arrest associated with focal degenerative orchitis in related dogs. J. Small Anim. Pract. 23, 337-343.

Cambrosio Mann M., Friess AE. and Stoffel M.H. (2003). Blood-tissue barriers in the male reproductive tract of the dog: a morphological study using lanthanum nitrate as an electron-opaque tracer. Cells Tissues Organs 174, 162-169.

Casal M.L. (2012). Canine autoimmune orchitis. Clin. Theriogenology. 4, 251-254.

Cheng C.Y., Wong E.W.P., Yan H.H.N. and Mruk D.D. (2010). Review: Regulation of spermatogenesis in the microenvironment of the seminiferous epithelium: New insights and advances. Mol. Cell Endocrinol. 315, 49-56.

Chihara M., Ikebuchi R., Otsuka S., Ichii O., Hashimoto Y., Suzuki A., Saga Y. and Kon Y. (2013). Mice stage-specific claudin 3 expression regulates progression of meiosis in early stage spermatocytes. Biol. Reprod. 89, 1-12.

Cyr D.G., Gregory M., Dube E., Dufresne J., Chan P.T. and Hermo L. (2007). Orchestration of occludins, claudins, catenins and cadherins as players involved in maintenance of the blood-epididymal barrier in animals and humans. Asian J. Androl. 9, 463-475.

Davidson A.P., von Dehn B.J. and Schlafer D.H. (2015). Adult-onset lymphoplasmacytic orchitis in a labrador retriever stud dog. Top. Companion Anim. Med. 30, 31-34.

Doncel G.F., Di Paola J.A. and Lustig L. (1989). Sequential study of the histopathology and cellular and humoral immune response during the development of an autoimmune orchitis in Wistar rats. Am. J. Reprod. Immunol. 20, 44-51.

Donnelly C.G., Soon Hon C. and Gilbert R.O. (2016). Unilateral autoimmune orchitis with concurrent contralateral testicular atrophy in a two-year-old Newfoundland dog. Vet. Rec. Case Rep. 4, e000277.

Dym M. and Romrell L.J. (1975). Intraepithelial lymphocytes in the male reproductive tract of rats and rhesus monkeys. J. Reprod. Fertil. 42, 1-7.

Egger G.F. and Witter K. (2009). Peritubular contractile cells in testis and epididymis of the dog, Canis lupus familiaris. Acta Veterinaria Brno 78, 3-11.

Fijak M. and Meinhardt A. (2006). The testis in immune privilege. Immunol. Rev. 213, 66-81.

Fijak M., Iosub R., Schneider E., Linder M., Respondek K., Klug J. and Meinhardt A. (2005). Identification of immunodominant autoantigens in rat autoimmune orchitis. J. Pathol. 207, 127-138.

Fink C., Weigel R., Fink L., Wilhelm J., Kliesch S., Zeiler M., Bergmann M. and Brehm R. (2009). Claudin-11 is over-expressed and dislocated from the blood-testis barrier in Sertoli cells associated with testicular intraepithelial neoplasia in men. Histochem. Cell Biol. 131, 755-764.

Fritz T.E., Lombard L.S., Tyler S.A. and Norris W.P. (1976). Pathology and familial incidence of orchitis and its relation to thyroiditis in a closed beagle colony. Exp. Mol. Pathol. 24, 142-158.

Gow A., Southwood C.M., Li J.S., Pariali M., Riordan G.P., Brodie S.E., Danias J., Bronstein J.M., Kachar B. and Lazzarini RA. (1999). CNS myelin and Sertoli cell tight junction strands are absent in Osp/claudin-11 null mice. Cell 99, 649-659.

Gregory M. and Cyr D.G. (2006). Identification of multiple claudins in the rat epididymis. Mol. Reprod. Dev. 73, 580-588.

Grieco V., Rondena M., Romussi S., Stefanello D. and Finazzi M. (2004). Immunohistochemical characterization of the leucocytic infiltrate associated with canine seminomas. J. Comp. Pathol. 130, 278-284.

Günzel-Apel A-R and Bostedt H. (2016). Hoden und Nebenhoden. In: Reproduktionsmedizin und Neonatologie von Hund und Katze. 1st ed. Schattauer. Stuttgart, Germany. pp 661-676.

Gye M.C. (2004). Expression of occludin in canine testis and epididymis. Reprod. Domest. Anim. 39, 43-47.

Hammer S.C., Becker A., Rateitschak K., Mohr A., Luder Ripoli F., Hennecke S., Junginger J., Hewicker-Trautwein M., Brenig B., Ngezahayo A., Nolte I. and Escobar H.M. (2016). Longitudinal claudin gene expression analyses in canine mammary tissues and thereof derived primary cultures and cell lines. Int. J. Mol. Sci. 17, 1655.

Hedger M.P. and Meinhardt A. (2003). Cytokines and the immune-testicular axis. J. Reprod. Immunol. 58, 1-26.

Hesser A.C. and Davidson A.P. (2015). Spermatocele in a south african boerboel dog. Top. Companion Anim. Med. 30, 28-30.

Jakab C., Halasz J., Szasz A.M., Kiss A., Schaff Z., Rusvai M., Galfi P. and Kulka J. (2008). Expression of claudin-1, -2, -3, -4, -5 and -7 proteins in benign and malignant canine mammary gland epithelial tumours. J. Comp. Pathol. 139, 238-245.

Mazaud-Guittot S., Meugnier E., Pesenti S., Wu X., Vidal H., Gow A. and Le Magueresse-Battistoni B. (2010). Claudin 11 deficiency in mice results in loss of the Sertoli cell epithelial phenotype in the testis. Biol. Reprod. 82, 202-213.

Memon M.A. (2007). Common causes of male dog infertility. Theriogenology 68, 322-328.

Meng J., Holdcraft R.W., Shima J.E., Griswold M.D. and Braun R.E. (2005). Androgens regulate the permeability of the blood-testis barrier. Proc. Natl. Acad. Sci. USA 102, 16696-16700.

Naito M., Terayama H., Hirai S., Qu N., Lustig L. and Itoh M. (2012). Experimental autoimmune orchitis as a model of immunological male infertility. Med. Mol. Morphol. 45, 185-189.

Ohta H., Yamaguchi T., Rajapakshage BK., Murakami M., Sasaki N., Nakamura K., Hwang SJ., Yamasaki M. and Takiguchi M. (2011). Expression and subcellular localization of apical junction proteins in canine duodenal and colonic mucosa. Am. J. Vet. Res. 72, 1046-1051.

Olson P.N., Schultheiss P. and Seim H.B. (1992). Clinical and laboratory findings associated with actual or suspected azoospermia in dogs: 18 cases (1979-1990). Am. Vet. Med. Assoc. 201, 478-482.

Pelletier R.M., Akpovi C.D., Chen L., Day R. and Vitale M.L. (2011). CX43 expression, phosphorylation, and distribution in the normal and autoimmune orchitic testis with a look at gap junctions joining germ cell to germ cell. Am. J. Physiol. Regul. Integr. Comp. Physiol. 300, 121-139.

Perez C.V., Sobarzo C., Jacobo P.V., Jarazo Dietrich S., Theas M., Denduchis B. and Lustig L. (2011). Impaired expression and distribution of adherens and gap junction proteins in the seminiferous tubules of rats undergoing autoimmune orchitis. Int. J. Androl. 34, e566-577.

Perez C.V., Sobarzo C.M., Jacobo P.V., Pellizzari E.H., Cigorraga S.B., Denduchis B. and Lustig L. (2012). Loss of occludin expression and impairment of blood-testis barrier permeability in rats with autoimmune orchitis: effect of interleukin 6 on Sertoli cell tight junctions. Biol. Reprod. 87, 1-12.

Perez C.V., Pellizzari E.H., Cigorraga S.B., Galardo M.N., Naito M., Lustig L. and Jacobo P.V. (2014). IL17A impairs blood-testis barrier integrity and induces testicular inflammation. Cell Tissue Res. 358, 885-898.

Pointis G. and Segretain D. (2005). Role of connexin-based gap junction channels in testis. Trends Endocrinol. Metab. 16, 300-306.

Ruttinger C., Bergmann M., Fink L., Pesch S., Seitz K, Trautmann A., Steger K., Konrad L. and Brehm R. (2008). Expression of connexin 43 in normal canine testes and canine testicular tumors. Histochem. Cell Biol. 130, 537-548.

Silva CA., Cocuzza M., Carvalho J.F. and Bonfa E. (2014). Diagnosis and classification of autoimmune orchitis. Autoimmun. Rev. 13, 431-434.

Smith B.E. and Braun R.E. (2012). Germ cell migration across Sertoli cell tight junctions. Science 338, 798-802.

Stammler A., Luftner B.U., Kliesch S., Weidner W., Bergmann M., Middendorff R. and Konrad L. (2016). Highly conserved testicular localization of claudin-11 in normal and impaired spermatogenesis. PLoS One 11, e0160349.

Stanton P.G. (2016). Regulation of the blood-testis barrier. Semin. Cell. Dev. Biol. 59, 166-173.

Suidan G.L., McDole J.R., Chen Y., Pirko I. and Johnson A.J. (2008). Induction of blood brain barrier tight junction protein alterations by CD8 T cells. PLoS One 3, e3037.

Tung K.S.K., Unanue E.R. and Dixon F.J. (1971). Pathogenesis of experimental allergic orchitis II. The role of antibody. J. Immunol. 106, 1463-1472.